

**Simultaneous generation of two spin-wave–photon entangled states in an atomic ensemble**Yuelong Wu, Long Tian, Zhongxiao Xu, Wei Ge, Lirong Chen, Shujing Li, Haoxiang Yuan, Yafei Wen, Hai Wang,\*  
Changde Xie, and Kunchi Peng*The State Key Laboratory of Quantum Optics and Quantum Optics Devices, Collaborative Innovation Center of Extreme Optics,  
Institute of Opto-Electronics, Shanxi University, Taiyuan 030006, People's Republic of China*

(Received 25 August 2015; revised manuscript received 18 December 2015; published 19 May 2016)

Spontaneous Raman scattering (SRS) in atomic ensembles provides a promising method to generate spin-wave–photon entangled states. In the past experiments, a spin-wave–photon entangled state was produced via SRS from an atomic ensemble. Here, we report a scheme of simultaneously generating two spin-wave–photon (atom-photon) entangled states in a cold Rb ensemble via SRS. Based on joint Bell-state measurements on the two photons coming from the two atom-photon entangled sources, respectively, we projected the two stored spin waves into a Bell state and then mapped the quantum memory into a polarization-entangled photon pair. Such a polarization-entangled photon pair can be released on demand and thus the presented scheme has potential application in the preparation of large-size photonic entangled states.

DOI: [10.1103/PhysRevA.93.052327](https://doi.org/10.1103/PhysRevA.93.052327)**I. INTRODUCTION**

The multiphoton entangled states are the crucial resources in one-way linear optical quantum computations (LOQC) [1–3]. Spontaneous parametric down-conversion (SPDC) is a common process used for generating polarization-entangled photon pairs [3]. By combining several polarization-entangled photon pairs on multiphoton interferometers, three-, six-, and eight-photon Greenberger-Horne-Zeilinger (GHZ) entangled states have been experimentally generated [4–7]. However, the probability of generating a pair of entangled photons from SPDC has to be far less than 1 (i.e.,  $\chi \ll 1$ ) in order to suppress the multiphoton generation [3]. The scalability of generating multiphoton entangled states [3] based on SPDC is limited since the preparations of such states require multiple entangled photon pairs simultaneously arriving at the interferometers [3]. For overcoming the limit, a promising scheme is to effectively store the randomly generated entangled-photon pairs in an atomic or solid-state ensemble and then release them at the same time [3].

The linewidth of the entangled photons from SPDC is on the order of several THz [8–10], which is beyond the linewidth of available atomic memories [9,10]. By means of the cavity-enhanced SPDC process, Pan's group has prepared narrowband polarization-entangled photon pairs [10]. Subsequently, the group has successfully stored one photon [11] and two photons [12] of such a pair in an atomic ensemble via dynamic electromagnetically induced transparency (EIT), respectively, with a storage lifetime of  $\sim 1 \mu\text{s}$ .

Spontaneous Raman scattering (SRS) in an atomic ensemble provides a hopeful method to achieve the quantum memory for polarization-entangled photon pairs. In the SRS process, a pair of correlated excitations, one spin-wave emission and a single photon, is created at the same time [9,13]. The correlation between the emitted photons and the spin-wave (collective) excitations forms the physical mechanism of

generating the entanglement between a photonic and an atomic qubit [9]. In the past decade, many experiments accomplished the generation of the spin-wave–photon (atom-photon) entanglement sources via SRS [14–20]. Based on such entanglement sources, several experiments have demonstrated the quantum memories for polarization-entangled two photons in two separated atomic ensembles with a distance of a few meters or few hundred meters [14,16,20], respectively.

In this paper, we present an experimental demonstration of simultaneously generating two spin-wave–photon (atom-photon) entangled states in a cold atomic ensemble. The generation of the entangled sources relies on SRS induced by write laser pulses, which simultaneously creates a single Stokes photon and one spin-wave excitation in certain spatial modes. Two orthogonal spin waves (SWs) associated with different Zeeman-sublevel coherences are utilized to encode an atomic qubit. In this way, the interferometric stability between the two SW modes required in Refs. [14,19,20] is not needed, and thus the experimental complexity is significantly reduced. Although in Refs. [15–18], the atomic qubits are also encoded in two SWs associated with different Zeeman-sublevel coherences, the excitations between the two SWs are unbalanced. In our experiment, by selecting an appropriate light-atom coupling scheme [see Fig. 1(c)], the two SWs are balanced and thus the entanglement quality is improved. The measured Bell parameters for the two spin-wave–photon entangled states are  $2.77 \pm 0.01$  and  $2.64 \pm 0.01$ , respectively. Based on the two obtained spin-wave–photon entangled states, we prepare the quantum memory for a pair of polarization-entangled photons according to the following steps: at first, sending the two single photons, respectively, coming from the two atom-photon entangled states to a polarization beam splitter (PBS) for two-photon detection, then projecting the two stored SWs into a Bell state conditioned on detecting a two-photon coincidence. After a storage time, we convert the quantum memory into a pair of polarization-entangled photons. Also, based on the two atom-photon entangled states, we generate a GHZ entangled state of three photons with a programmable delay.

\*wanghai@sxu.edu.cn

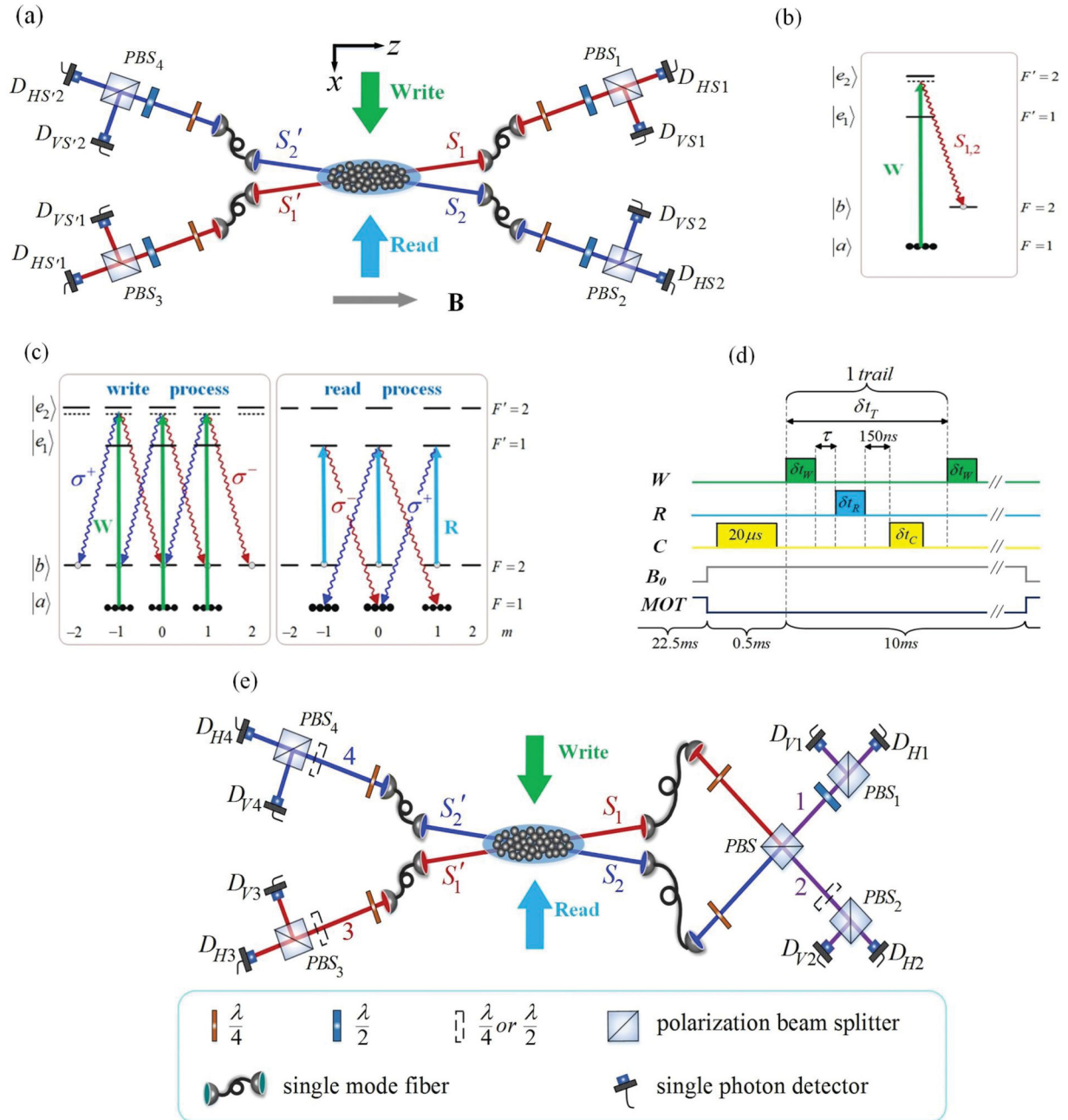


FIG. 1. Overview of the experiment. (a) Experimental setup of two atom-photon entangled states. The magnetic field  $B = 200$  mG is applied on the cold atoms along the  $z$  axis. The  $z$ -polarized write beam goes through the atoms along the  $x$  direction, while the  $z$ -polarized read beam counterpropagates with respect to the write beam. (b, c) Relevant atomic levels without and with considering Zeeman sublevels. (d) The time sequence of an experimental cycle. (e) Experimental setup for generating either polarization-entangled photon pairs or three-photon GHZ entanglement.

## II. THEORETICAL MODEL FOR THE ATOM-PHOTON ENTANGLED STATE

The experimental setup and relevant atomic levels for generating two independent spin-wave-photon entangled states are shown in Figs. 1(a)–1(e). A cloud of cold  $^{87}\text{Rb}$  atoms [see Figs. 1(a) and 1(e)] loaded by a two-dimensional magneto-optical trap (MOT) serves as the media for quantum memory. A weak magnetic field is applied along the  $z$  direction to define the quantum axis. The cold atoms are prepared in

the initial state  $|a\rangle$  and then a  $z$ -polarized writing laser pulse with 10 MHz red-detuned to  $|a\rangle \rightarrow |e_2\rangle$  transition is applied onto the atoms. Without considering Zeeman sublevels [see Fig. 1(b)], the write pulse will induce a spontaneous Raman transition  $|a\rangle \rightarrow |b\rangle$  via  $|e_2\rangle$ , in which Stokes photons are emitted and spin-wave excitations are created at the same time. If a single Stokes photon is collected and detected in a spatial mode  $S_i$  at a small angle ( $\pm 0.4^\circ$  for  $i = 1, 2$  in the presented experiment) relative to the  $z$  axis, a single SW

excitation correlated with the single photon will be generated in the spatial mode  $A_i$ . The wave vector of the SW mode  $A_i$  is  $\vec{k}_{A_i} = \vec{k}_w - \vec{k}_{S_i}$ , where  $\vec{k}_w$  and  $\vec{k}_{S_i}$  are the wave vectors of the write field and the Stokes field  $S_i$ , respectively.

If the Zeeman sublevels [Fig. 1(c)] are considered, the entanglement between the atomic and the photonic qubits will be observed. Assuming that the atoms are initially prepared in the  $|a, m_a\rangle$  state ( $m_a = 0, \pm 1$ ), two spontaneous Raman

transitions will occur: one is  $|a, m_a\rangle \rightarrow |b, m_b = m_a - 1\rangle$  via  $|e_2, m_a\rangle$ , which generates a correlated pair of a single  $\sigma^+$ -polarized Stokes photon in the  $S_i$  mode and a SW excitation  $|\psi^{m_a, m_b=m_a-1}\rangle$  in the  $A_i$  mode and another one is  $|a, m_a\rangle \rightarrow |b, m_b = m_a + 1\rangle$  via  $|e_2, m_a\rangle$ , which generates a correlated pair of a single  $\sigma^-$ -polarized Stokes photon in the  $S_i$  mode and one SW excitation  $|\psi^{m_a, m_b=m_a+1}\rangle$  in the  $A_i$  mode. The SW is represented by

$$|\psi^{m_a, m_b}\rangle_{A_i} = \hat{s}_\alpha^\dagger(m_a)|0\rangle_{A_i} = \sqrt{\frac{2F_a + 1}{N}} \sum_{j=1}^{N_m} |a_1^{m_a}\rangle_{A_i} \dots |b_j^{m_b=m_a+\alpha}\rangle_{A_i} \dots |a_{N_m}^{m_a}\rangle_{A_i} e^{-\vec{k}_{A_i} \cdot \vec{r}_j}, \quad (1)$$

which is associated with the coherence  $|a, m_a\rangle \leftrightarrow |b, m_b = m_a + \alpha\rangle$ , where  $\hat{s}_\alpha^\dagger(m_a) = \sqrt{\frac{2F_a+1}{N}} \sum_j |b^{m_a+\alpha}\rangle_j \langle a^{m_a}|_j |0\rangle_{A_i} = \otimes^j |a\rangle_{A_i}^j = \otimes^j |a^{m_a=-1}\rangle_{A_i}^j \otimes^j |a^{m_a=0}\rangle_{A_i}^j \otimes^j |a^{m_a=1}\rangle_{A_i}^j$  denote the vacuum states of the spin-wave mode  $A_i$ ;  $\alpha = \pm 1$  represents photon helicity;  $N$  is the number of atoms, which are assumed to be prepared in  $|a\rangle$  with equal probability in the three Zeeman sublevels  $|m_a = -1\rangle, |m_a = 0\rangle$ , and  $|m_a = 1\rangle$ ; i.e.,  $N_{m_a} = N/(2F_a + 1)$ ,  $F_a = 1$ . The emission of a single  $\sigma^+$ -polarized Stokes photon will create the SW:

$$\begin{aligned} |\psi\rangle_{A_i}^+ &= \hat{s}_+^\dagger|0\rangle_{A_i} = \left[ \frac{X_{+1}(-1)}{X_{+1}} \hat{s}_+^\dagger(-1) + \frac{X_{+1}(0)}{X_{+1}} \hat{s}_+^\dagger(0) + \frac{X_{+1}(1)}{X_{+1}} \hat{s}_+^\dagger(1) \right] |0\rangle_{A_i} \\ &= [X_{+1}(-1)|\psi^{-1,0}\rangle_{A_i} + X_{+1}(0)|\psi^{0,1}\rangle_{A_i} + X_{+1}(1)|\psi^{1,2}\rangle_{A_i}] / X_{+1}, \end{aligned} \quad (2)$$

while the emission of a  $\sigma^-$ -polarized Stokes photon will create the SW:

$$\begin{aligned} |\psi\rangle_{A_i}^- &= \hat{s}_-^\dagger|0\rangle_{A_i} = \left[ \frac{X_{-1}(-1)}{X_{-1}} \hat{s}_-^\dagger(-1) + \frac{X_{-1}(0)}{X_{-1}} \hat{s}_-^\dagger(0) + \frac{X_{-1}(1)}{X_{-1}} \hat{s}_-^\dagger(1) \right] |0\rangle_{A_i} \\ &= [X_{-1}(-1)|\psi^{-1,-2}\rangle_{A_i} + X_{-1}(0)|\psi^{0,-1}\rangle_{A_i} + X_{-1}(1)|\psi^{1,0}\rangle_{A_i}] / X_{-1}, \end{aligned} \quad (3)$$

where,  $X_\alpha(m_a) = C_{m_a, 0, m_a}^{F_a, 1, F_{e_2}} C_{m_a, \alpha, m_a + \alpha}^{F_{e_2}, 1, F_b}$  is the product of the relevant Clebsch-Gordan coefficient for the transition [15]  $X_\alpha^2 = X_\alpha^2(m_a = 1) + X_\alpha^2(m_a = 0) + X_\alpha^2(m_a = -1)$ . Considering that the SWs  $|\psi^{1,2}\rangle_{A_i}$  and  $|\psi^{-1,-2}\rangle_{A_i}$  cannot be retrieved in the reading process [see Fig. 1(c)], we neglect them and rewrite  $X_\alpha$  and the SWs  $|\psi\rangle_{A_i}^\pm$  as

$$X_{\pm 1}^2 = X_{\pm 1}^2(\pm 1) + X_{\pm 1}^2(0), \quad (4a)$$

$$|\psi\rangle_{A_i}^+ = \left[ \frac{X_{+1}(-1)}{X_{+1}} |\psi^{-1,0}\rangle_{A_i} + \frac{X_{+1}(0)}{X_{+1}} |\psi^{0,1}\rangle_{A_i} \right], \quad (4b)$$

$$|\psi\rangle_{A_i}^- = \left[ \frac{X_{-1}(0)}{X_{-1}} |\psi^{0,-1}\rangle_{A_i} + \frac{X_{-1}(1)}{X_{-1}} |\psi^{1,0}\rangle_{A_i} \right], \quad (4c)$$

respectively. Under the condition of the excitation probability  $\chi \ll 1$ , the atom-photon joint state can be written as  $\rho_{S_i-A_i} = |0\rangle_{S_i-A_i} \langle 0| + |\Phi\rangle_{S_i-A_i} \langle \Phi|$ , where the vacuum state  $|0\rangle_{S_i-A_i} = |0\rangle_{S_i} |0\rangle_{A_i}$ ,  $|0\rangle_{S_i}$  denotes the vacuum state of the Stokes light mode  $S_i$ ; the nonvacuum part  $|\Phi\rangle_{S_i-A_i}$  is

$$\begin{aligned} |\Phi\rangle_{S_i-A_i} &= \chi (\cos \vartheta \hat{s}_+^\dagger \hat{a}_L^\dagger + \sin \vartheta \hat{s}_-^\dagger \hat{a}_R^\dagger) |0\rangle_{S_i} |0\rangle_{A_i} + O(\chi^2) \\ &= \chi (\cos \vartheta |\psi\rangle_{A_i}^+ |L\rangle_{S_i} + \sin \vartheta |\psi\rangle_{A_i}^- |R\rangle_{S_i}) + O(\chi^2), \end{aligned} \quad (5)$$

and the parameters  $\cos \vartheta = \frac{\sqrt{X_{-1}^2}}{\sqrt{X_{-1}^2 + X_{+1}^2}}$  and  $\sin \vartheta = \frac{\sqrt{X_{+1}^2}}{\sqrt{X_{-1}^2 + X_{+1}^2}}$ . According to values of Clebsch-Gordan coefficient for the

transitions of  $^{87}\text{Rb}$  atoms, we calculate  $\frac{X_{+1}(-1)}{X_{+1}} = \sqrt{\frac{3}{7}}$ ,  $\frac{X_{+1}(0)}{X_{+1}} = \sqrt{\frac{4}{7}}$ ,  $\frac{X_{-1}(0)}{X_{-1}} = \sqrt{\frac{4}{7}}$ , and  $\frac{X_{-1}(1)}{X_{-1}} = \sqrt{\frac{3}{7}}$ . Thus we obtain  $\cos \vartheta = \frac{\sqrt{X_{-1}^2}}{\sqrt{X_{-1}^2 + X_{+1}^2}} = \sqrt{\frac{1}{2}}$  and  $\sin \vartheta = \frac{\sqrt{X_{+1}^2}}{\sqrt{X_{-1}^2 + X_{+1}^2}} = \sqrt{\frac{1}{2}}$ , respectively, which show that the collective excitations between the two SWs  $|\psi\rangle_{A_i}^+$  and  $|\psi\rangle_{A_i}^-$  are symmetric. So, in the case of neglecting the higher-order excitations, the entanglement between the photonic and atomic qubits is the maximally entangled state:

$$|\Phi\rangle_{S_i-A_i} = (|\psi\rangle_{A_i}^+ |L\rangle_{S_i} + |\psi\rangle_{A_i}^- |R\rangle_{S_i}) / \sqrt{2}, \quad (6)$$

where  $|R\rangle_{S_i} = \hat{a}_R^\dagger |0\rangle_{S_i}$ , ( $|L\rangle_{S_i} = \hat{a}_L^\dagger |0\rangle_{S_i}$ ) represents a  $\sigma^+$ - ( $\sigma^-$ ) polarized single photon state. In the presented experimental setup [see Fig. 1(a)], we collect the Stokes photons in the  $S_1$  ( $S_2$ ) mode by using a single-mode optical fiber. After the fiber, we transform the  $\sigma^+/\sigma^-$ -polarized state of the  $S_1$  ( $S_2$ ) photon into the vertically (horizontally)  $|V\rangle$  ( $|H\rangle$ ) polarized state by placing a  $\lambda/4$  plate in their paths. After a storage time  $\tau$ , the atom-photon entanglement state becomes

$$|\Phi(\tau)\rangle_{S_i-A_i} = \frac{1}{\sqrt{2}} (|H\rangle_{S_i} |\psi(\tau)\rangle_{A_i}^+ + |V\rangle_{S_i} |\psi(\tau)\rangle_{A_i}^-), \quad (7)$$

where

$$|\psi(\tau)\rangle_{A_i}^+ = \left[ \sqrt{\frac{3}{7}} e^{-i\beta\tau} |\psi_{A_i}^{-1,0}(0)\rangle + \sqrt{\frac{4}{7}} e^{i\beta\tau} |\psi_{A_i}^{0,1}(0)\rangle \right], \quad (8a)$$

$$|\psi(\tau)\rangle_{A_i}^- = \left[ \sqrt{\frac{4}{7}} e^{-i\beta\tau} |\psi_{A_i}^{0,-1}(0)\rangle + \sqrt{\frac{3}{7}} e^{i\beta\tau} |\psi_{A_i}^{1,0}(0)\rangle \right]. \quad (8b)$$

$\beta = g\mu_B B/\hbar$  is the phase shift due to Larmor precessions of the spin waves in the magnetic field  $B$ . The atom-photon entanglement state  $|\Phi(\tau)\rangle_{S_i-A_i}$  can be rewritten as

$$|\Phi(\tau)\rangle_{S_i-A_i} = \frac{1}{\sqrt{2}} (|H\rangle_{S_i} |\psi\rangle_{A_i}^+ + e^{-i\zeta(\tau)} |V\rangle_{S_i} |\psi\rangle_{A_i}^-), \quad (9)$$

where the phase shift  $\zeta(\tau) = 2 \arctan \frac{(\sqrt{4/7}-\sqrt{3/7}) \sin \beta t}{(\sqrt{4/7}+\sqrt{3/7}) \cos \beta t}$ , which will reduce the quality of the entangled states. However, for the presented experiment, we perform the polarization correlation measurements in the storage time range of  $\tau = 0 - 500$  ns; and the phase shift is very small [ $\zeta(\tau) \leq 3^\circ$ ] in this time range, which allows us to neglect it in the entangled state  $|\Psi(\tau)\rangle_{S_i-A_i}$ .

$$E(\theta_{s_i}, \theta_{as_i}) = \frac{C_{HS_i, HS_i'}(\theta_{s_i}, \theta_{as_i}) + C_{VS_i, VS_i'}(\theta_{s_i}, \theta_{as_i}) - C_{HS_i, VS_i'}(\theta_{s_i}, \theta_{as_i}) - C_{VS_i, HS_i'}(\theta_{s_i}, \theta_{as_i})}{C_{HS_i, HS_i'}(\theta_{s_i}, \theta_{as_i}) + C_{VS_i, VS_i'}(\theta_{s_i}, \theta_{as_i}) + C_{HS_i, VS_i'}(\theta_{s_i}, \theta_{as_i}) + C_{VS_i, HS_i'}(\theta_{s_i}, \theta_{as_i})}. \quad (11)$$

For example,  $C_{HS_i, HS_i'}(\theta_{s_i}, \theta_{as_i})$  is the number of coincidences between the detectors  $D_{HS_i}$  and  $D_{HS_i'}$ ;  $\theta_{s_i}$  and  $\theta_{as_i}$  are the polarization angles of the Stokes photon  $S_i$  and anti-Stokes photon  $S_i'$ , respectively.

### III. EXPERIMENTAL GENERATION OF ATOM-PHOTON ENTANGLED STATES

As shown in Fig. 1(a), the cold atomic cloud in the two-dimensional MOT consists of  $\sim 10^{987}$  Rb atoms, whose size, temperature, and optical density are  $\sim 5 \times 2 \times 2$  mm<sup>3</sup>,  $\sim 130$   $\mu$ K, and about 7, respectively. The atoms are optically pumped into the initial level  $|a\rangle$  by using  $\sigma^\pm$ -polarized laser beams  $P_1$  and  $P_2$  [not shown in Fig. 1(a)], which are overlapped at a polarization beam splitter and then collinearly go through the atoms at an angle of  $2^\circ$  to the  $z$  axis. The frequencies of  $P_1$  and  $P_2$  are tuned on the  $|b\rangle \leftrightarrow |e_2\rangle$  and  $|b\rangle \leftrightarrow |e_1\rangle$  transitions, respectively, and the power of both  $P_1$  and  $P_2$  is kept at  $\sim 60$  mW. The write and read beams counterpropagate through the atoms along the  $x$  axis, whose diameters (powers) in the MOT are  $\sim 3$  mm (1 mW) and 3.3 mm ( $\sim 50$  mW), respectively.

The experiments of generating the atom-photon entangled states are carried out in a cyclic fashion with a repeating frequency of 30 Hz. As shown in Fig. 1(d), each experimental cycle contains a 23-ms preparation stage and a 10-ms experiment run. During the preparation stage, the atomic ensembles are trapped in the MOT for 22 ms and further cooled by Sisyphus cooling for 0.5 ms. Then the MOT (beams and magnetic field) is turned off and the guiding magnetic field  $B = 200$  mG is applied. At the end of this stage,  $P_1$  and  $P_2$  laser beams are switched on for 20  $\mu$ s to pump the atoms into the level  $|a\rangle$ . After the preparation stage, the 10-ms experiment runs which contains  $n$  trails. In each trail, a write laser pulse with a length of  $\delta t_W = 70$  ns is applied to generate correlated

At time  $\tau$ , we apply a strong read laser pulse resonating with atomic  $|b\rangle \rightarrow |e_1\rangle$  transition to map the SW  $|\psi\rangle_{A_i}^+$  ( $|\psi\rangle_{A_i}^-$ ) into a  $\sigma^+$ - ( $\sigma^-$ ) polarized anti-Stokes photon in the  $S_i'$  mode. The  $S_i'$  mode has the wave vector of  $\vec{k}_i' = -\vec{k}_i$  under the condition of the counterpropagation of write and read beams [see Fig. 1(a)]. We also collect the anti-Stokes photons in the  $S_1'$  ( $S_2'$ ) mode by using a single-mode optical fiber and place a  $\lambda/4$  plate after the fiber to transform the  $R/L$  basis into the  $H/V$  basis. The entangled state between the Stokes and anti-Stokes photons is written as

$$|\Phi(\tau)\rangle_{S_i'-S_i} = \frac{1}{\sqrt{2}} (|H\rangle_{S_i'} |H\rangle_{S_i} + |V\rangle_{S_i'} |V\rangle_{S_i}). \quad (10)$$

The quality of the entangled state  $|\Phi\rangle_{S_i'-S_i}$  can be judged by the Bell–Clauser–Horne–Shimony–Holt (Bell-CHSH) inequality [21]:  $S_i^{\text{CHSH}} = |E(\theta_{s_i}, \theta_{as_i}) - E(\theta_{s_i}, \theta'_{as_i}) + E(\theta'_{s_i}, \theta_{as_i}) + E(\theta'_{s_i}, \theta'_{as_i})| < 2$ , where the correlation function  $E(\theta_{s_i}, \theta_{as_i})$  is given by

pairs of a single Stokes photon and a single SW excitation. After a storage time  $\tau$ , a read laser pulse with a length of  $\delta t_R = 100$  ns is applied to retrieve the stored SWs. At the end of each trail, the atoms are pumped back to the  $|a\rangle$  by switching on the laser beams  $P_1$  and  $P_2$  for a duration time of  $\delta t_c = 200$  ns. For the case of  $\tau = 30$  ns ( $\tau = 230, 430$  ns), the 10-ms experimental run contains  $n = 10\,000$  ( $n = 8333$ ) trails, thus a 1-s experimental sequence contains  $N = 300\,000$  ( $N = 24\,990$ ) trails. The total detection efficiencies for detecting the photons  $S_1, S_2, S_1'$ , and  $S_2'$  in Fig. 1(a) are  $\eta_{S_1} \approx \eta_{S_2} \approx \eta_{S_1'} \approx \eta_{S_2'} \approx 30\%$ , which include the transmissions of the optical filters (80%), the coupling efficiency of fiber coupler (80%), the efficiency of fiber coupling to the single-photon detectors (95%), and the quantum efficiency of the single-photon detectors (50%). The efficiencies of the two SWs  $A_1$  and  $A_2$  converted into the photons  $S_1'$  and  $S_2'$  are  $R_3 \approx R_4 \approx 20\%$  for the storage time of  $\tau = 30$  ns. The excitation probability in the presented experiment is set at  $\chi \approx 0.014$ . In the case of the canonical settings  $\theta_{s_i} = 0^\circ, \theta_{as_i} = 22.5^\circ, \theta'_{s_i} = 45^\circ$ , and  $\theta'_{as_i} = 67.5^\circ$ , we measure  $E(\theta_{s_i}, \theta_{as_i})$  and then obtain the Bell parameters, which are  $S_1^{\text{CHSH}} = 2.77 \pm 0.01$  ( $2.75 \pm 0.01$ ) and  $S_2^{\text{CHSH}} = 2.64 \pm 0.01$  ( $2.67 \pm 0.01$ ) for the storage time of  $\tau = 30$  ns (230 ns), respectively; both of them significantly violate the Bell-CHSH inequality  $|S^{\text{CHSH}}| < 2$ . The measured generation rates for the entangled photon pairs  $S_1/S_1'$  and  $S_2/S_2'$  are  $\sim 60$ /s at  $\tau = 30$  ns.

### IV. QUANTUM MEMORY FOR A POLARIZATION-ENTANGLED PHOTON PAIR

By means of joint Bell-state measurements on the two Stokes photons coming from the two entangled sources  $|\Phi\rangle_{S_i-A_i}$ , respectively, we project the two stored SWs  $A_1$  and  $A_2$  into a Bell state and then obtain quantum memory for a

TABLE I. Measured correlation function  $E(\theta_3, \theta_4)$  of the entangled photons 3 and 4 conditioned on observing a coincidence event at the detectors  $D_{H1}/D_{H1}$  or  $D_{V2}/D_{V2}$  for several different storage times  $\tau$ . The errors represent  $\pm 1$  standard deviation, which are estimated from Poissonian detection statistics using Monte Carlo simulation.

		$E(\theta_3, \theta_4)$		
$\theta_3$	$\theta_4$	30 ns	230 ns	430 ns
0°	22.5°	0.55 ± 0.06	0.55 ± 0.06	0.63 ± 0.07
0°	67.5°	-0.66 ± 0.05	-0.66 ± 0.06	-0.58 ± 0.07
45°	22.5°	0.57 ± 0.06	0.43 ± 0.06	0.27 ± 0.08
45°	67.5°	0.63 ± 0.05	0.61 ± 0.06	0.58 ± 0.07
		$S^{\text{CHSH}} = 2.40 \pm 0.12$	$S^{\text{CHSH}} = 2.28 \pm 0.12$	$S^{\text{CHSH}} = 2.06 \pm 0.15$

polarization-entangled photon pair. As shown in Fig. 1(e), the two Stokes photons  $S_1$  and  $S_2$  are overlapped on a polarization beam splitter (PBS) of transmitting  $H$  and reflecting  $V$  polarization to perform a two-photon interference. If the two Stokes photons are in the same polarization  $H$  or  $V$ , they will exit from two different output ports of the PBS. Thus, a four-particle entangled state will be formed [22], which is written as

$$|\Psi\rangle_{G4} = \frac{1}{\sqrt{2}}(|\psi\rangle_{A_1}^+ |\psi\rangle_{A_2}^+ |H\rangle_1 |H\rangle_2 + |\psi\rangle_{A_1}^- |\psi\rangle_{A_2}^- |V\rangle_1 |V\rangle_2), \quad (12)$$

where the subscripts 1 and 2 denote the emitting photons from the two output ports. The four-particle entanglement state  $|\Psi\rangle_{G4}$  can be expressed as

$$|\Psi\rangle_{G4} = \frac{1}{2}(|\Phi\rangle_{A_1 A_2}^+ |\varphi\rangle_{12}^+ + |\Phi\rangle_{A_1 A_2}^- |\varphi\rangle_{12}^-), \quad (13)$$

where  $|\Phi\rangle_{A_1 A_2}^\pm = \frac{1}{\sqrt{2}}(|\psi\rangle_{A_1}^+ |\psi\rangle_{A_2}^+ \pm |\psi\rangle_{A_1}^- |\psi\rangle_{A_2}^-)$ ,  $|\varphi\rangle_{12}^\pm = (|H'\rangle_1 |H'\rangle_2 + |V'\rangle_1 |V'\rangle_2)/\sqrt{2}$ , and  $|\varphi\rangle_{12}^\pm = (|H'\rangle_1 |V'\rangle_2 + |V'\rangle_1 |H'\rangle_2)/\sqrt{2}$  are the Bell states;  $|H'\rangle = (|H\rangle + |V\rangle)/\sqrt{2}$  and  $|V'\rangle = (|H\rangle - |V\rangle)/\sqrt{2}$  correspond to  $+45^\circ$  and  $-45^\circ$  linear polarizations, respectively. The state  $|\varphi\rangle_{12}^\pm$  can be identified by a suitable joint polarization measurement on photons 1 and 2. As shown in Fig. 1(e), two  $\lambda/2$  plates are inserted in the paths of modes 1 and 2 to rotate the polarizations of photons 1 and 2 by  $45^\circ$ , respectively. So, the measurements of linear polarization  $H'/V'$  on photon 1 (2) will be implemented by detector  $D_{H1}/D_{V1}$  ( $D_{H2}/D_{V2}$ ). Conditioned on detecting a two-photon coincidence at detectors  $D_{H1}$  and  $D_{H2}$  or  $D_{V1}$  and  $D_{V2}$ , photons 1 and 2 are projected into the Bell state  $|\varphi\rangle_{12}^\pm$  [23] and thus the SWs in the  $A_1$  and  $A_2$  modes will be projected onto the entangled state:

$$|\Phi\rangle_{A_1 A_2}^\pm = \frac{1}{\sqrt{2}}(|\psi\rangle_{A_1}^+ |\psi\rangle_{A_2}^+ + |\psi\rangle_{A_1}^- |\psi\rangle_{A_2}^-). \quad (14)$$

After a storage time  $\tau$ , a read laser pulse is applied to transfer the entangled SWs  $|\Phi\rangle_{A_1 A_2}^\pm$  into the polarization-entangled state of photons 3 and 4:

$$|\Phi\rangle_{34} = \frac{1}{\sqrt{2}}(|H\rangle_3 |H\rangle_4 + |V\rangle_3 |V\rangle_4). \quad (15)$$

Actually, there are double excitations in either the spin-wave mode  $A_1$  or  $A_2$ , which will induce error events in the Bell-state measurements and then reduce the creation probability of the entangled state  $|\Phi\rangle_{A_1 A_2}^\pm$  to  $\frac{1}{2}$  (See Ref. [20,24]

or Appendix for details). The error events can be eliminated at the stage of entanglement verification of the state  $|\Phi\rangle_{A_1 A_2}^\pm$  by the fourfold coincidence of photons 1, 2, 3, and 4 [9,20,24].

For characterizing the quality of the polarization-entangled two-photon state  $|\Phi\rangle_{34}$ , we measure correlation functions  $E(\theta_3, \theta_4)$  between photons 3 and 4 by using detectors  $D_3$  ( $D_{H3}/D_{V3}$ ) and  $D_4$  ( $D_{H4}/D_{V4}$ ), where  $\theta_3$  and  $\theta_4$  are the polarization angles of photons 3 and 4, respectively. The measured results are shown in Table I. We then obtain the Bell parameter through  $S^{\text{CHSH}} = |E(\theta_3, \theta_4) - E(\theta'_3, \theta_4) + E(\theta_3, \theta'_4) + E(\theta'_3, \theta'_4)|$ . In Table I, we list the measured correlation  $E(\theta_3, \theta_4)$  and Bell parameter  $S^{\text{CHSH}}$  for three values of storage time  $\tau$ : 30, 230 ns, and 430 ns. At  $\tau = 30$  ns, we obtain a maximal value of  $S^{\text{CHSH}} = 2.40 \pm 0.12$ , which violates Bell-CHSH inequality by  $\sim 3.3$  standard deviations. The measured rate for the pair of entangled photons 3 and 4 conditioned on detecting the coincidence event in the detectors  $D_{H1}$  and  $D_{H2}$  or  $D_{V1}$  and  $D_{V2}$  is  $R_{3,4} \approx 22/\text{h}$  for  $\tau = 30$  ns, while the measured rate of the coincidence in the detectors  $D_{H1}$  and  $D_{H2}$  or  $D_{V1}$  and  $D_{V2}$  is  $C_{1,2} \approx 1.78 \times 10^4/\text{h}$ . So, the detection probability of the entangled photons 3 and 4 conditioned on detecting the coincidence event in the detectors  $D_{H1}$  and  $D_{H2}$  or  $D_{V1}$  and  $D_{V2}$  is  $r_{34} = R_{3,4}/C_{1,2} \approx 1.24 \times 10^{-3}$ . The preparation probability of polarization-entangled photons 3 and 4 conditioned on detecting the coincidence event in the detectors  $D_{H1}$  and  $D_{H2}$  or  $D_{V1}$  and  $D_{V2}$  is defined by  $r_{34}^p = R_3 R_4 / 2$ , where the factor of  $\frac{1}{2}$  is the limit of the probability to project the two spin waves into a Bell state;  $R_3$  and  $R_4$  are conversion efficiencies of the two SWs ( $A_1$  and  $A_2$ ) into photons 3 and 4, respectively. The relation between the detection and the preparation probabilities is  $r_{34} = r_{34}^p \eta_{D3} \eta_{D4}$ , where  $\eta_{D3}$  and  $\eta_{D4}$  are overall efficiencies of the  $D_3$  and  $D_4$  channels, respectively. For the presented experimental setup,  $\eta_{D3} \approx \eta_{D4} \approx 0.3$ , so we have  $r_{34}^{\text{int}} \approx 1.4 \times 10^{-2}$ , which is far below the theoretical limit of  $\frac{1}{2}$  because of the imperfect retrieval efficiencies of  $R_3$  and  $R_4$ .

The quality of the two-photon entangled state can be also characterized by the state fidelity  $F$ , which is defined by  $F = \text{Tr}(\sqrt{\sqrt{\rho} \rho_{\text{ideal}} \sqrt{\rho}})^2$ , where  $\rho$  ( $\rho_{\text{ideal}}$ ) is the reconstructed (ideal) density matrices of the entangled state. By performing the measurements on the two photons 3 and 4 in  $H/V$ ,  $H'/V'$ , and  $R/L$  [ $R = (H + iV)/\sqrt{2}$  and  $L = (H - iV)/\sqrt{2}$ ] bases, we reconstructed the density matrices  $\rho$  for three values of storage time: 30, 230, and 430 ns, which are shown in Figs. 2(a)–2(c), respectively. From the density matrices  $\rho$ , we then give the state fidelities  $F$  for the three times, which are shown

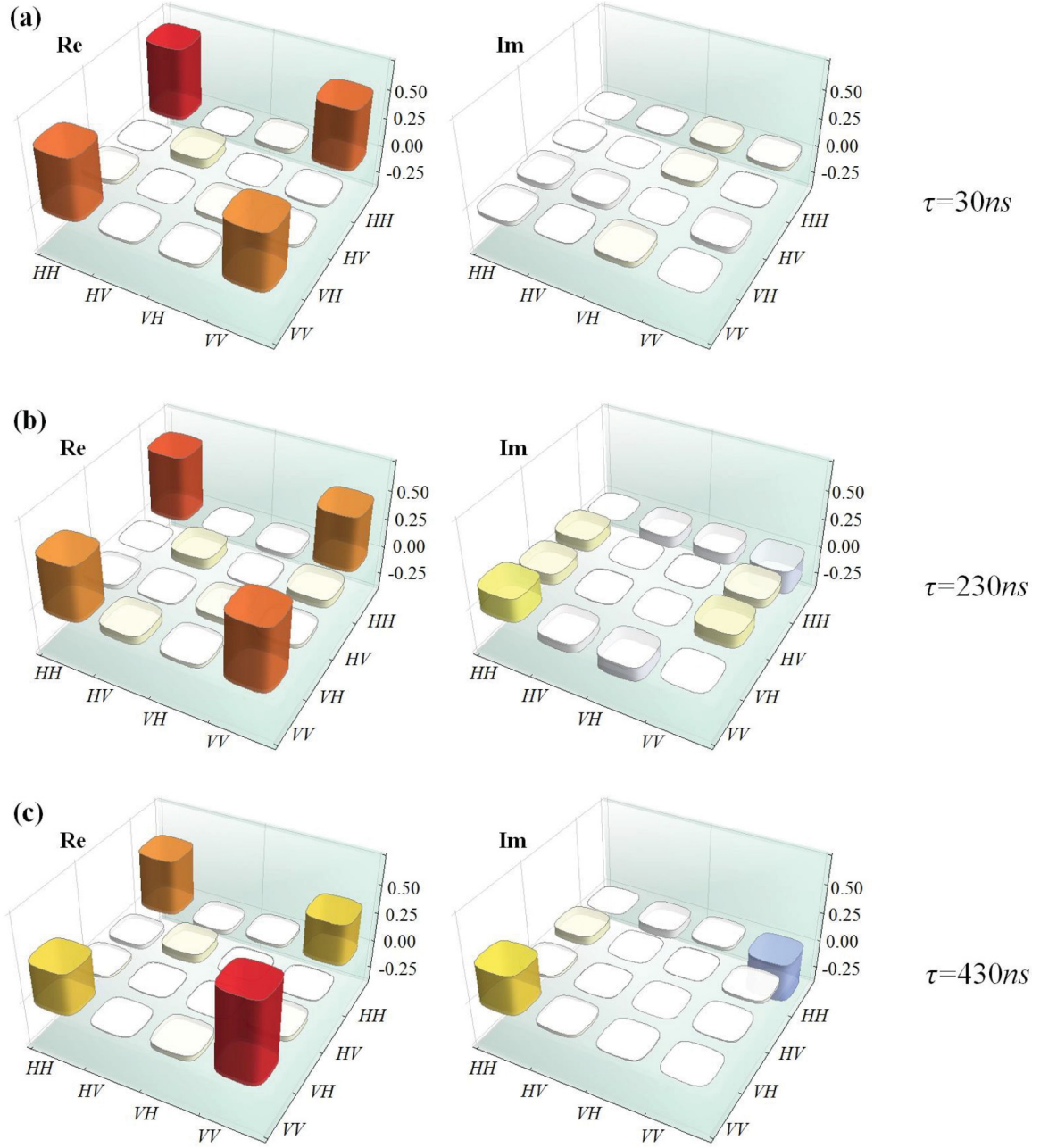


FIG. 2. Real and imaginary parts of the reconstructed density matrices of the polarization-entangled two-photon states for three values of storage time  $\tau$ : (a) 30, (b) 230, and 430 ns.

in Table II. From Table II, we see that for  $\tau = 230$  ns,  $F = 82.4 \pm 2.2\%$  with two standard deviations beyond the limit of 78% [25].

TABLE II. Measured fidelity of the entangled photons 3 and 4. The errors represent  $\pm 1$  standard deviation, which are estimated from Poissonian detection statistics using Monte Carlo simulation.

	30 ns	230 ns	430 ns
Fidelity	$87.1 \pm 2.0\%$	$82.4 \pm 2.2\%$	$76.9 \pm 3.7\%$

### V. THREE-PHOTON GHZ ENTANGLED STATE

Based on the two atom-photon entangled sources, we next demonstrate the generation of three-photon GHZ entanglement by performing a suitable polarization measurement on photon 1. As shown in Fig. 1(e), the polarization of photon 1 is rotated by  $45^\circ$  with the  $\lambda/2$  plate at the front of the PBS. In this case, if  $D_{1H}$  registers a photon, photon 1 is projected into the polarization state  $|H'\rangle$  and at the same time, the four-particle entangled state is projected into a tripartite GHZ entangled state:

$$|\Psi\rangle_{G3} = \frac{1}{\sqrt{2}}(|\psi\rangle_{A_1}^+ |\psi\rangle_{A_2}^+ |H\rangle_2 + |\psi\rangle_{A_1}^- |\psi\rangle_{A_2}^- |V\rangle_2). \quad (16)$$

TABLE III. Measured witness and Mermin correlations of three-photon GHZ entangled state for  $\tau = 30$  ns. The errors represent  $\pm 1$  standard deviation, which are estimated from Poissonian detection statistics using Monte Carlo simulation.

$E(\sigma_z^{(2)}, \sigma_z^{(3)})$	$0.92 \pm 0.03$	$E(\sigma_x^{(2)}, \sigma_y^{(3)}, \sigma_y^{(4)})$	$-0.80 \pm 0.05$
$E(\sigma_z^{(3)}, \sigma_z^{(4)})$	$0.89 \pm 0.03$	$E(\sigma_y^{(2)}, \sigma_x^{(3)}, \sigma_y^{(4)})$	$-0.77 \pm 0.05$
$E(\sigma_x^{(2)}, \sigma_z^{(4)})$	$0.94 \pm 0.02$	$E(\sigma_y^{(2)}, \sigma_y^{(3)}, \sigma_x^{(4)})$	$-0.77 \pm 0.05$
$E(\sigma_x^{(2)}, \sigma_x^{(3)}, \sigma_x^{(4)})$	$0.80 \pm 0.04$	$E(\sigma_x^{(2)}, \sigma_x^{(3)}, \sigma_x^{(4)})$	$-0.80 \pm 0.04$

After a storage time  $\tau$ , the spin waves  $|\psi\rangle_{A_1}^+$  and  $|\psi\rangle_{A_1}^-$  ( $|\psi\rangle_{A_2}^+$  and  $|\psi\rangle_{A_2}^-$ ) are retrieved into photonic polarization states  $|H\rangle_3$  and  $|V\rangle_3$  ( $|H\rangle_4$  and  $|V\rangle_4$ ) by dynamic EIT and the tripartite GHZ state is transferred into a three-photon GHZ entangled state:

$$|\Psi\rangle_{G3} = \frac{1}{\sqrt{2}}(|H\rangle_2|H\rangle_3|H\rangle_4 + |V\rangle_2|V\rangle_3|V\rangle_4). \quad (17)$$

To evaluate the quality of the entangled state, we apply the two-setting witness [26]:

$$W_{\text{GHZ3}} = \frac{3}{2}I^{\otimes 3} - \sigma_x^{(2)}\sigma_x^{(3)}\sigma_x^{(4)} - \frac{1}{2}(\sigma_z^{(2)}\sigma_z^{(3)} + \sigma_z^{(3)}\sigma_z^{(4)} + \sigma_z^{(2)}\sigma_z^{(4)}), \quad (18)$$

where  $I$  is a two-dimensional identity matrix;  $\sigma_x^{(2)}\sigma_x^{(3)}\sigma_x^{(4)}$  represents a joint measurement of linear polarization  $H'/V'$  on photons 2, 3, and 4;  $\sigma_z^{(2)}\sigma_z^{(3)}$  ( $\sigma_z^{(3)}\sigma_z^{(4)}$ ,  $\sigma_z^{(2)}\sigma_z^{(4)}$ ) denotes a joint measurement of linear polarization  $H/V$  on photons 2 and 3 (3 and 4, 2 and 4). If the measured witness is a negative value, the tripartite will be in the GHZ entangled state [26]. The measured expectation values of the observables  $E(\sigma_x^{(2)}\sigma_x^{(3)}\sigma_x^{(4)})$ ,  $E(\sigma_z^{(2)}\sigma_z^{(3)})$ ,  $E(\sigma_z^{(3)}\sigma_z^{(4)})$ ,  $E(\sigma_z^{(2)}\sigma_z^{(4)})$  conditioned on detecting a photon at detector  $D_{1H}$  are listed in Table III; each expectation value is deduced from 160 to 190 fourfold-coincidence events. Note that the detecting time of photons 1 and 2 is earlier than that of photons 3 and 4 by a storage time  $\tau = 30$  ns. Substituting these data into Eq. (18), we obtain  $\langle W_{\text{GHZ3}} \rangle = -0.68 \pm 0.10$ , which confirms that the three photons are in the genuine GHZ entanglement state. The lower bound for the GHZ-state fidelity calculated with Eq. (47) in Ref. [26] is  $F \geq \frac{1}{2} - \frac{1}{2}\langle W_{\text{GHZ3}} \rangle = 0.84 \pm 0.05$ .

For demonstrating the conflict between local realism and quantum mechanics for the GHZ entanglement, we use the Mermin inequality of the tripartite [27]:

$$S_{\text{Mermin}} = |E(\sigma_y^{(2)}, \sigma_y^{(3)}, \sigma_x^{(4)}) + E(\sigma_y^{(2)}, \sigma_x^{(3)}, \sigma_y^{(4)}) + E(\sigma_x^{(2)}, \sigma_y^{(3)}, \sigma_y^{(4)}) - E(\sigma_x^{(2)}, \sigma_x^{(3)}, \sigma_x^{(4)})| \leq 2, \quad (19)$$

where, for example,  $E(\sigma_y^{(2)}, \sigma_y^{(3)}, \sigma_x^{(4)})$  is the expectation value of the measurement setting  $\sigma_y^{(2)}\sigma_y^{(3)}\sigma_x^{(4)}$ , which represents the joint measurement of circular polarization  $R/L$  on photons 1 and 2 and linear polarization  $H'/V'$  on photon 3. The measured expectation values  $E(\sigma_y^{(2)}, \sigma_y^{(3)}, \sigma_x^{(4)})$ ,  $E(\sigma_y^{(2)}, \sigma_x^{(3)}, \sigma_y^{(4)})$ ,  $E(\sigma_x^{(2)}, \sigma_y^{(3)}, \sigma_y^{(4)})$ , and  $E(\sigma_x^{(2)}, \sigma_x^{(3)}, \sigma_x^{(4)})$  conditioned on detecting a photon at detector  $D_{1H}$  are shown in Table III; each value is also deduced from 160 to 190 fourfold-coincidence events. From the measured data, we obtain the Mermin parameter of  $S_{\text{Mermin}} = 3.14 \pm 0.12$ , which violates the limit of the local realism by nine standard

deviations. Because we use Pauli measurements in the Mermin inequality, this violation also confirms that three photons are in a genuine GHZ entangled state. The conclusion is correct for the imperfect  $\sigma_x$  and  $\sigma_y$  measurements, since the measured Mermin parameter  $S_{\text{Mermin}}$  is larger than the limit of the device-independent witness of genuine tripartite entanglement of  $2\sqrt{2}$  [27].

## VI. CONCLUSION

In conclusion, we simultaneously produce two spin-wave-photon entangled states in a cold atomic ensemble via SRS. Using the obtained spin-wave-photon entangled states as quantum resources, we achieve the quantum memory for a pair of polarization-entangled photons and prepare a GHZ entangled state of three photons with a programmable delay, respectively. Although the realized memory lifetime is only on the order of a submicrosecond, if a Bose-Einstein condensate atomic medium is available, we believe that the memory lifetime can be improved to  $\sim 0.5$  ms [28,29]. The lower retrieval efficiencies in the presented experiment can be enhanced by increasing the optical depth of the cold atoms [30] or coupling the atoms into an optical cavity [18,31]. The realized quantum memory allows us to release a pair of polarization-entangled photons on demand, which has potential application in the preparation of large-size photonic entangled states [3].

## ACKNOWLEDGMENTS

We acknowledge funding support from the 973 Program (Grant No. 2010CB923103), the National Natural Science Foundation of China (Grants No. 11475109, No. 11274211, and No. 60821004).

## APPENDIX

Considering the double excitations, the atom-photon entangled state  $|\Phi\rangle_{S_i-A_i}$  in Eq. (5) in the text should be rewritten as

$$|\Phi\rangle_{S_i-A_i} = \chi(\hat{s}_+^\dagger \hat{a}_L^\dagger + \hat{s}_-^\dagger \hat{a}_R^\dagger)|0\rangle_{S_i}|0\rangle_{A_i} + \frac{\chi^2}{2}\hat{s}_+^\dagger \hat{s}_-^\dagger \hat{a}_L^\dagger \hat{a}_R^\dagger|0\rangle_{S_i}|0\rangle_{A_i}, \quad (A1)$$

where the first part is the atom-photon entangled state used for building the entangled states  $|\Phi\rangle_{A_1 A_2}^+$ , which has been discussed in the above; the second part represents the unwanted double excitations coming from second-order excitations, which correspond to the events that both  $\sigma^+$ - and  $\sigma^-$ -polarized Stokes photons emit into either of the  $S_1$  or  $S_2$  modes. The two  $\sigma^+$ - and  $\sigma^-$ -polarized Stokes photons can be split by the PBS as shown in Fig. 1(e) and then directed into 1 and 2 modes, respectively. Thus a four-particle state due to the double excitations is formed, which is given by

$$|\Psi\rangle'_{G4} = \frac{\chi^2}{2}(|\psi\rangle_{A_1}^+ |\psi\rangle_{A_1}^- |V\rangle_1 |H\rangle_2 + |\psi\rangle_{A_2}^+ |\psi\rangle_{A_2}^- |H\rangle_1 |V\rangle_2) = \frac{\chi^2}{2}[|DD\rangle_{A_1 A_2}^+ |\phi\rangle_{12}^- + |DD\rangle_{A_1 A_2}^- |\phi\rangle_{12}^-], \quad (A2)$$

where  $|DD\rangle^\pm = \frac{1}{\sqrt{2}}(|\psi\rangle_{A_1}^+|\psi\rangle_{A_2}^- + |\psi\rangle_{A_2}^+|\psi\rangle_{A_1}^-)$  are the unwanted SW double-excitation states,  $|\phi\rangle_{12}^- = (|H'\rangle_1|H'\rangle_2 - |V'\rangle_1|V'\rangle_2)/\sqrt{2}$  and  $|\phi\rangle_{12}^+ = (|H'\rangle_1|V'\rangle_2 - |V'\rangle_1|H'\rangle_2)/\sqrt{2}$ .

Combining the contributions of the first and second parts in Eq. (A1), we obtain the total four-particle state, which is

$$\begin{aligned} |\Psi\rangle_{G4}^T &= |\Psi\rangle_{G4} + |\Psi\rangle_{G4}' \\ &= \frac{\chi^2}{2}(|\Phi\rangle_{A_1A_2}^+|\phi\rangle_{12}^+ + |DD\rangle_{A_1A_2}^+|\phi\rangle_{12}^-) \\ &\quad + \frac{\chi^2}{2}(|\Phi\rangle_{A_1A_2}^-|\phi\rangle_{12}^+ + |DD\rangle_{A_1A_2}^-|\phi\rangle_{12}^-). \end{aligned} \quad (\text{A3})$$

From the total four-particle state, we can see that coincidence events between detectors  $D_{H1}$  and  $D_{H2}$  or  $D_{V1}$  and  $D_{V2}$  [see Fig. 1(e)] will project photons 1 and 2 into either the  $|\phi\rangle_{12}^+$  or  $|\phi\rangle_{12}^-$  Bell state and thus the two SWs  $A_1$  and  $A_2$  are projected onto the state

$$|\Phi\rangle_{A_1A_2}^+ + |DD\rangle_{A_1A_2}^+. \quad (\text{A4})$$

Since the probabilities of the first and second terms in Eq. (A4) are equal to each other, so the creation probability of the entangled state  $|\Phi^+\rangle_{A_1A_2}$  under the condition of detecting one two-photon coincidence event is  $\frac{1}{2}$ .

- 
- [1] H. J. Briegel, D. E. Browne, W. Dür, R. Raussendorf, and M. Van den Nest, *Nat. Phys.* **5**, 19 (2009).
- [2] D. E. Browne and T. Rudolph, *Phys. Rev. Lett.* **95**, 010501 (2005).
- [3] J.-W. Pan, Z.-B. Chen, C.-Y. Lu, H. Weinfurter, A. Zeilinger, and M. Żukowski, *Rev. Mod. Phys.* **84**, 777 (2012).
- [4] J.-W. Pan, D. Bouwmeester, M. Daniell, H. Weinfurter, and A. Zeilinger, *Nature* **403**, 515 (2000).
- [5] C.-Y. Lu, X.-Q. Zhou, O. Gühne, W.-B. Gao, J. Zhang, Z.-S. Yuan, A. Goebel, T. Yang, and J.-W. Pan, *Nat. Phys.* **3**, 91 (2007).
- [6] X.-C. Yao, T.-X. Wang, P. Xu, H. Lu, G.-S. Pan, X.-H. Bao, C.-Z. Peng, C.-Y. Lu, Y.-A. Chen, and J.-W. Pan, *Nat. Photonics* **6**, 225 (2012).
- [7] Y.-F. Huang, B.-H. Liu, L. Peng, Y.-H. Li, L. Li, C.-F. Li, and G.-C. Guo, *Nat. Commun.* **2**, 546 (2011).
- [8] C. Clausen, I. Usmani, F. Bussières, N. Sangouard, M. Afzelius, H. de Riedmatten, and N. Gisin, *Nature* **469**, 508 (2011).
- [9] N. Sangouard, C. Simon, H. de Riedmatten, and N. Gisin, *Rev. Mod. Phys.* **83**, 33 (2011).
- [10] X.-H. Bao, Y. Qian, J. Yang, H. Zhang, Z.-B. Chen, T. Yang, and J.-W. Pan, *Phys. Rev. Lett.* **101**, 190501 (2008).
- [11] H. Zhang, X.-M. Jin, J. Yang, H.-N. Dai, S.-J. Yang, T.-M. Zhao, J. Rui, Y. He, X. Jiang, F. Yang, G.-S. Pan, Z.-S. Yuan, Y. Deng, Z.-B. Chen, X.-H. Bao, S. Chen, B. Zhao, and J.-W. Pan, *Nat. Photonics* **5**, 628 (2011).
- [12] H.-N. Dai, H. Zhang, S.-J. Yang, T.-M. Zhao, J. Rui, Y.-J. Deng, L. Li, N.-L. Liu, S. Chen, X.-H. Bao, X.-M. Jin, B. Zhao, and J.-W. Pan, *Phys. Rev. Lett.* **108**, 210501 (2012).
- [13] L. M. Duan, M. D. Lukin, J. I. Cirac, and P. Zoller, *Nature (London)* **414**, 413 (2001).
- [14] D.-S. Ding, W. Zhang, Z.-Y. Zhou, S. Shi, B.-S. Shi, and G.-C. Guo, *Nat. Photonics* **10**, 1038 (2015).
- [15] D. N. Matsukevich, T. Chanelière, M. Bhattacharya, S.-Y. Lan, S. D. Jenkins, T. A. B. Kennedy, and A. Kuzmich, *Phys. Rev. Lett.* **95**, 040405 (2005).
- [16] D. N. Matsukevich, T. Chanelière, S. D. Jenkins, S.-Y. Lan, T. A. B. Kennedy, and A. Kuzmich, *Phys. Rev. Lett.* **96**, 030405 (2006).
- [17] H. de Riedmatten, J. Laurat, C. W. Chou, E. W. Schomburg, D. Felinto, and H. J. Kimble, *Phys. Rev. Lett.* **97**, 113603 (2006).
- [18] S.-J. Yang, X.-J. Wang, J. Li, J. Rui, X.-H. Bao, and J.-W. Pan, *Phys. Rev. Lett.* **114**, 210501 (2015).
- [19] S. Chen, Y.-A. Chen, B. Zhao, Z.-S. Yuan, J. Schmiedmayer, and J.-W. Pan, *Phys. Rev. Lett.* **99**, 180505 (2007).
- [20] Z.-S. Yuan, Y.-A. Chen, B. Zhao, S. Chen, J. Schmiedmayer, and J.-W. Pan, *Nature* **454**, 1098 (2008).
- [21] J. F. Clauser, M. A. Horne, A. Shimony, and R. A. Holt, *Phys. Rev. Lett.* **23**, 880 (1969).
- [22] Z. Zhao, T. Yang, Y.-A. Chen, A.-N. Zhang, M. Żukowski, and J.-W. Pan, *Phys. Rev. Lett.* **91**, 180401 (2003).
- [23] J.-W. Pan and A. Zeilinger, *Phys. Rev. A* **57**, 2208 (1998).
- [24] B. Zhao, Z.-B. Chen, Y.-A. Chen, J. Schmiedmayer, and J.-W. Pan, *Phys. Rev. Lett.* **98**, 240502 (2007).
- [25] M. Aspelmeyer, H. R. Böhm, T. Gyatso, T. Jennewein, R. Kaltenbaek, M. Lindenthal, G. Molina-Terriza, A. Poppe, K. Resch, M. Taraba, R. Ursin, P. Walther, and A. Zeilinger, *Science* **301**, 621 (2003).
- [26] G. Tóth and O. Gühne, *Phys. Rev. A* **72**, 022340 (2005).
- [27] N. D. Mermin, *Phys. Rev. Lett.* **65**, 1838 (1990).
- [28] M. Lettner, M. Mücke, S. Riedl, C. Vo, C. Hahn, S. Baur, J. Bochmann, S. Ritter, S. Dürr, and G. Rempe, *Phys. Rev. Lett.* **106**, 210503 (2011).
- [29] S. Riedl, M. Lettner, C. Vo, S. Baur, G. Rempe, and S. Dürr, *Phys. Rev. A* **85**, 022318 (2012).
- [30] J. Laurat, H. de Riedmatten, D. Felinto, C.-W. Chou, E. W. Schomburg, and H. J. Kimble, *Opt. Express* **14**, 6912 (2006).
- [31] M. Afzelius and C. Simon, *Phys. Rev. A* **82**, 022310 (2010).